Polarimetric Method for Ice Water Content Determination

A. V. RYZHKOV

Cooperative Institute for Mesoscale Meteorological Studies, University of Oklahoma, Norman, Oklahoma

D. S. ZRNIC

National Severe Storms Laboratory, Norman, Oklahoma

B. A. GORDON

Cooperative Institute for Mesoscale Meteorological Studies, University of Oklahoma, Norman, Oklahoma

(Manuscript received 2 October 1996, in final form 26 June 1997)

ABSTRACT

Two variants of a polarimetric method to determine ice water content are presented. One uses specific differential phase and differential reflectivity and the other uses specific differential phase; both quantities are for a 10-cm wavelength. Theoretical considerations indicate that these polarimetric methods are suited for pristine ice crystals. Ice water content of lightly to moderately aggregated crystals might also be estimated. Verification of the proposed method is made using in situ data collected by the T-28 instrumented aircraft. Comparison with two estimators that use the reflectivity factor suggests that the polarimetric methods are better and can quantify correctly ice water content in the range above 0.1 g m^{-3}.

1. Introduction

There have been a number of studies to estimate ice water content (IWC) of snow clouds using radar reflectivity factor Z [e.g., starting from early works of Sekhon and Srivastava (1970); Heymsfield (1977); and others]. A review of different IWC–Z relations is given by Sassen (1987), and a recent paper by Atlas et al. (1995) summarizes the results obtained for cirrus clouds. All of these studies show extreme variability in the IWC–Z relations, which appear to vary from day to day and cloud to cloud. Furthermore, substantial differences in these relations exist for different reflectivity ranges. Thus, the relations obtained for cirrus clouds, with a reflectivity factor usually under 5 dBZ, are quite different from those for snowfall with reflectivities up to 45 dBZ. High diversity in the IWC–Z relations is primarily due to the fact that the reflectivity factor is proportional to the product of IWC and mass of average-sized ice hydrometeor; therefore, at least one more independent measurement is needed to resolve this ambiguity.

Because ice and snow hydrometeors are nonspherical, use of polarimetry is a natural way for estimation of bulk properties of snow clouds. Matrosov et al. (1996) explore elliptical depolarization ratio at Ka band (8-mm wavelength) as a function of an antenna elevation angle in an attempt to distinguish between various types of ice crystals. Vivekanandan et al. (1994) suggest use of specific differential phase K_{DP} to estimate IWC and claim that K_{DP} is not sensitive to size distribution; hence, it might be used for IWC estimation, provided that the average density and axis ratio of the ice crystals are known. However, the latter provision is seldom, if ever, fulfilled. Vivekanandan et al. (1994) model crystals as oblate spheroids. Aydin and Tang (1995) discuss the possibility to derive IWC of the cloud composed of pristine crystals from combined measurements of K_{DP} and differential reflectivity Z_{DR} with a stipulation that the density of crystals is equal to the density of ice.

Polarimetric data in snow (Vivekanandan et al. 1994; Ryzhkov and Zrnic 1995) indicate that at least for reflectivities below 35 dBZ, distinct signatures in the fields of K_{DP} and Z_{DR} usually exist and can be recognized.

In this paper we develop a radar polarimetric model for a cloud of ice hydrometeors and obtain a polarimetric relation for computing IWC. We account for the diversity of crystal shapes and use reported assumptions on the shape and density of scatterers as a function of their size (Matrosov et al. 1996). Eleven categories of ice crystals are considered with different dependencies of shapes and densities on the size. We examined the performance of the proposed polarimetric method for estimating IWC using in situ data collected by the T-28 instrumented aircraft in Oklahoma.

2. Assumptions

We model ice particles as oblate and prolate spheroids with axes a and b, where axis a is the axis of rotation.

Corresponding author address: Dr. A. V. Ryzhkov, NSSL/CIMMS, 1313 Halley Circle, Norman, OK 73069.
E-mail: ryzhkov@nssla.nssl.uoknor.edu

TABLE 1. The coefficients α and β for different classes of crystals.

Crystal class	α	β
1. Dendrites	0.038	0.377
2. Solid thick plates	0.230	0.778
3. Hexagonal plates	0.047	0.474
4. Solid columns ($L/h \leq 2$)	0.637	0.958
5. Solid columns ($L/h > 2$)	0.308	0.927
6. Hollow columns ($L/h \leq 2$)	0.541	0.892
7. Hollow columns ($L/h > 2$)	0.309	0.930
8. Long solid columns	0.128	0.437
9. Solid bullets ($L \leq 0.3$ mm)	0.250	0.786
10. Hollow bullets ($L > 0.3$ mm)	0.185	0.532
11. Elementary needles	0.073	0.611

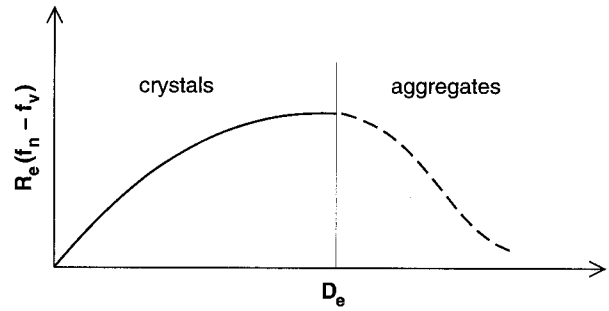

FIG. 1. Dependence of Re($f_h - f_v$) on the size of snow hydrometeor in the presence of aggregation.

Thus, $a < b$ for oblates and $a > b$ for prolates. The oblates are assumed oriented so that the axis of rotation is vertical, whereas prolates are considered to be randomly oriented in the horizontal plane.

We consider dry snow for which dielectric constant ε can be computed from the following relation (Matrosov et al. 1996):

$$\frac{\varepsilon - 1}{\varepsilon + 2} = \frac{\rho}{\rho_i}\frac{\varepsilon_i - 1}{\varepsilon_i + 2}, \tag{1}$$

where ρ is the density of snow, $\rho_i = 0.92$ g cm^{-3} is the density of dense ice, and ε_i is the dielectric constant of dense ice. We describe the density versus size relation in the transition from elementary pristine crystals to aggregates by the equation (Matrosov et al. 1996)

$$\rho = 0.07D^{-1.1}, \tag{2}$$

where D is the equivolume diameter of the particle. In (2) and throughout the paper, ρ is in grams per cubic centimeter and D is in millimeters. The relation (2) cited by Matrosov et al. (1996) was originally derived from the mass–size relation appropriate for ''aggregates of unrimed bullets, columns, and sideplanes'' given by Locatelli and Hobbs (1974). For pure crystals, Matrosov et al. (1996) in their Table 1 report very weak (if any) dependence of the bulk density on the crystal size. Recent studies, however, show that this probably applies only to small crystals with maximal dimensions less than 0.1–0.2 mm. For example, Kajikawa (1989), Mitchell et al. (1990), Detwiler et al. (1993), and Brown and Francis (1995) present evidence that the relation $M \sim L^2$, where M is a mass of particle and L is its maximal dimension, is approximately valid for both aggregates and crystals with $L > 0.1$–0.2 mm. Only part of this dependence could be caused by the change of the axis ratio with size, which decreases slightly [Fig. 1 in Matrosov (1991)]. We submit that most of the dependence is due to the change of ρ with size. Therefore, we apply relation (2) to all snow particles under consideration and then examine how the change in the $\rho(D)$ assumption affects our final results.

The shape of ice hydrometeors is highly variable. It depends on the type of crystal and its size. Following Matrosov et al. (1996), we consider 11 categories of ice particles (in Table 1) with distinctly different dependencies of their aspect ratios on size. The relation between the smaller and larger dimensions (h and L, respectively) of crystals can be expressed by the power law

$$h = \alpha L^{\beta}. \tag{3}$$

The coefficients α and β in (3) are listed in the second and third columns of Table 1 for h and L expressed in millimeters. Several investigators (Pruppacher and Klett 1978; Heymsfield 1972; Auer and Veal 1970; Jayaweera and Cottis 1969; Jayaweera and Ohtake 1974) have determined experimentally the coefficients α and β and a summary of these is in Matrosov et al. (1996). The plot of the aspect ratio for different types of crystals as a function of their size can be found in Matrosov (1991). Strictly, validity of (3) with the coefficients specified in Table 1 becomes questionable as crystals start to aggregate. Nevertheless, as aggregation proceeds, there is a rapid decrease of snow density, and therefore, polarimetric variables such as specific differential phase and differential reflectivity tend to be less affected by the shape. For that reason, convenience, and lack of a better relation, we apply (3) even to lightly or moderately aggregated crystals.

Note that contrary to our approach, Vivekanandan et al. (1994) assume no dependence of shape and density on the size of snow particles and consider oblate particles only.

3. Basic relations

The modeling is done in the Rayleigh approximation, and therefore, the final results are valid for at least the centimeter wavelengths. In the Rayleigh region, the scattering amplitudes of spheroidal particles in the forward and backward directions are equal and can be expressed as (van de Hulst 1981)

$$f_{a,b} = f_{a,b}(0) = f_{a,b}(\pi) = \frac{\pi^2 D^3}{6\lambda^2}\xi_{a,b'} \tag{4}$$

and

$$\xi_{a,b} = \frac{1}{L_{a,b} + \dfrac{1}{\varepsilon - 1}}, \tag{5}$$

where λ is the wavelength in millimeters, f_a is the scattering amplitude if the electric field vector is parallel to the axis of rotation of the hydrometeor, and f_b stands for the scattering amplitude if the electric vector is perpendicular to the axis of rotation. The parameter $L_{a,b}$ determines the shape of the hydrometeor. For the prolates, L_a is obtained from the formula

$$L_a = \frac{1 - e^2}{e^2}\left(\frac{1}{2e}\ln\frac{1 + e}{1 - e} - 1\right), \tag{6}$$

where $e = [1 - (b/a)^2]^{1/2}$. For the oblates, L_a is given by

$$L_a = \frac{1 + f^2}{f^2}\left(1 - \frac{\operatorname{arctg} f}{f}\right), \tag{7}$$

where $f = [(b/a)^2 - 1]^{1/2}$. Here, L_b is equal to $(1 - L_a)/2$.

The radar cross section $\sigma_{a,b}$ of a snow particle is

$$\sigma_{a,b} = 4\pi|f_{a,b}|^2 = \frac{\pi^5 D^6}{9\lambda^4}\xi_{a,b}^2. \tag{8}$$

We consider the case of hydrometeor illumination at low-elevation angles. The generalization for arbitrary elevations can be done easily. Thus, the expressions for radar reflectivity factors at orthogonal linear polarizations and specific differential phase are as follows:

$$Z_{h,v} = \frac{\lambda^4}{\pi^5 K^2}\int \sigma_{h,v} N(D)\, dD \tag{9}$$

and

$$K_{\mathrm{DP}} = \frac{180\lambda}{\pi}\int \mathrm{Re}(f_h - f_v) N(D)\, dD, \tag{10}$$

where $f_h = f_b$, $f_v = f_a$, $\sigma_h = \sigma_b$, and $\sigma_v = \sigma_a$ for oblate hydrometeors. In (9), $K = |(\varepsilon_w - 1)/(\varepsilon_w + 2)|$ and ε_w is the dielectric constant of water. The value of $Z_{h,v}$ is expressed in mm^6 m^{-3}, and K_{DP} is in degrees per kilometer.

For prolates randomly oriented in the horizontal plane,

$$f_v = f_b,$$

$$f_h = \langle f_a \cos^2\phi + f_b \sin^2\phi\rangle = 1/2(f_a + f_b), \tag{11}$$

where the brackets mean averaging over all azimuthal angles ϕ. Hence, $f_h - f_v = ½(f_a - f_b)$. Similarly,

$$\sigma_v = 4\pi f_b^2,$$

$$\sigma_h = 4\pi\langle f_h^2\rangle = 4\pi\left(3/8 f_a^2 + 1/4 f_a f_b + 3/8 f_b^2\right). \tag{12}$$

Our objective is to obtain the relation between IWC and radar variables Z_h, K_{DP}, and either $Z_{\mathrm{DP}} = Z_h - Z_v$ or $Z_{\mathrm{DR}} = Z_h/Z_v$ that are readily available if measurements are performed in linear vertical–horizontal polarization basis. First, we outline the strategy in a qualitative manner and then proceed with a more rigorous derivation.

It follows from (2) that the density ρ of the ice hydrometeor is usually quite low if its size is larger than 0.5 mm. At low densities, $\varepsilon - 1$ is roughly proportional to ρ, and $\varepsilon - 1 = \mu\rho$, where μ is a coefficient of proportionality. Furthermore, $L_{a,b} \ll 1/(\varepsilon - 1)$ in (5) and the expression for $\xi_{a,b}$ can be expanded as follows:

$$\xi_{a,b} \approx \mu\rho(1 - L_{a,b}\,\mu\rho). \tag{13}$$

At first approximation for oblate particles, $\sigma_h = \sigma_b \sim \rho^2 D^6 \sim M^2$, where M is the mass. Therefore, for a narrow interval of particle size (or mass M), the reflectivity factor is proportional to the product of particle concentration N and the square of mass $Z_h \sim NM^2$, whereas the IWC is proportional to the product of concentration and mass, IWC $\sim NM$. Both IWC and Z_h do not depend on the shape of ice hydrometeors. To estimate IWC, we need to determine N and M independently; thus, it is necessary to find an independent polarimetric parameter from which either N or M can be derived. Such a parameter could be the ratio $Z_{\mathrm{DP}}/K_{\mathrm{DP}}$, which can be written as

$$\frac{Z_{\mathrm{DP}}}{K_{\mathrm{DP}}} \sim \frac{D^6(\xi_b^2 - \xi_a^2)}{D^3(\xi_b - \xi_a)} = D^3(\xi_b + \xi_a) \sim \rho D^3 \sim M. \tag{14}$$

Note that both K_{DP} and Z_{DP} are highly dependent on the particle shape because $\xi_b - \xi_a \approx \mu^2\rho^2(L_a - L_b)$ according to (13), whereas their ratio does not depend on the shape and is determined only by the mass of the particle. Combining Z_h and $Z_{\mathrm{DP}}/K_{\mathrm{DP}}$, we obtain

$$\mathrm{IWC} \sim Z_h K_{\mathrm{DP}}/Z_{\mathrm{DP}} = K_{\mathrm{DP}}/(1 - Z_{\mathrm{DR}}^{-1}). \tag{15}$$

Thus, IWC can be estimated using K_{DP} and Z_{DR}. Next, we obtain the relation for IWC in a more rigorous manner.

Using formulas (4)–(8) and (11)–(12), we derive power-law relations between the mass of the particle M and the parameters σ_h and $\mathrm{Re}(f_h - f_v)$ for all 11 categories of hydrometeors, assuming the dependency of density on equivolume diameter defined by (2)

$$\sigma_h = \frac{\pi^5}{9\lambda^4}a_1 M^2 \tag{16}$$

and

$$\mathrm{Re}(f_h - f_v) = \frac{\pi^2}{6\lambda^2}a_2 M^{b_2}, \tag{17}$$

where M is expressed in milligrams. These relations are valid for a range of maximal size L of particles between 0 and 4 mm. The coefficients $a_{1,2}$ and b_2 are different for different categories of crystals. The exponents b_2 are between 0.48 and 0.58, which is at variance with the conclusion by Vivekanandan et al. (1994) that $\mathrm{Re}(f_h - f_v)$ is almost linearly proportional to the particle mass. This discrepancy is a consequence of different initial assumptions regarding shape and density of ice crystals. Remarkably, the ratio $(\sigma_h - \sigma_v)/\mathrm{Re}(f_h - f_v)$ is almost linearly proportional to the mass of the ice particle and is approximately given by

$$\frac{\sigma_h - \sigma_v}{\mathrm{Re}(f_h - f_v)} = \frac{2\pi^2}{3\lambda^3} a_3 M. \tag{18}$$

In (18), $a_3 \approx 5.2$ and practically does not depend on the type of ice crystals. Using (16)–(18) we arrive at the following formulas for Z_h, K_{DP}, and Z_{DP}:

$$Z_h = \frac{a_1}{9K^2} \int M^2 N(D)\, dD, \tag{19}$$

$$K_{\mathrm{DP}} = \frac{0.03\pi a_2}{\lambda} \int M^{b_2} N(D)\, dD, \tag{20}$$

and

$$Z_{\mathrm{DP}} = \frac{a_2 a_3}{9K^2} \int M^{b_2+1} N(D)\, dD. \tag{21}$$

The final goal is to establish a relation between the radar variables (19)–(21) and the ice water content:

$$\mathrm{IWC} = 10^{-3} \int MN(D)\, dD, \tag{22}$$

where IWC is expressed in grams per cubic meter. Assume that the particle size distribution $N(D)$ is exponential:

$$N(D) = \frac{N_0}{D_0} \exp\left(-\frac{D}{D_0}\right), \tag{23}$$

where D_0 is the mean hydrometeor diameter.

The relation between particle mass and its equivolume diameter is determined by (2) and can generally be written as $M = \gamma D^\delta$. The exponent δ is equal to 1.9 if the dependence of ρ on D is specified by (2). The integrals in (19)–(22) can be easily expressed via gamma functions:

$$\int M^\tau N(D)\, dD = N_0 M_0^\tau \Gamma(\delta\tau + 1), \tag{24}$$

where $M_0 = \gamma D_0^\delta$.

After integrations, we can write

$$Z_h = \frac{a_1 10^3}{9K^2} \frac{\Gamma(2\delta + 1)}{\Gamma(\delta + 1)} M_0 \mathrm{IWC}, \tag{25}$$

$$\frac{Z_{\mathrm{DP}}}{K_{\mathrm{DP}}} = \frac{\lambda a_3}{0.27\pi K^2} \frac{\Gamma[\delta(b_2 + 1) + 1]}{\Gamma(\delta b_2 + 1)} M_0, \tag{26}$$

and finally

$$\mathrm{IWC} = \frac{\lambda}{30\pi} C_1 \frac{K_{\mathrm{DP}}}{Z_{\mathrm{DP}}} Z_h, \tag{27}$$

where the coefficient C_1 is

$$C_1 \frac{a_3}{a_1} \frac{\Gamma(\delta + 1)}{\Gamma(2\delta + 1)} \frac{\Gamma[\delta(b_2 + 1) + 1]}{\Gamma(\delta b_2 + 1)}. \tag{28}$$

For a given value of $\delta = 1.9$, that is, for a fixed dependence of ρ on D, the average value of the coefficient C_1 is equal to 0.42 and appears to be quite stable; its fractional standard deviation is about 20% for all types of crystals examined. Variability of the $\rho(D)$ relation affects the coefficient C_1 through the coefficients a_1, b_2, and δ in (28), which depend on the exponent of the $\rho(D)$ power law relation. The change of the exponent within the range from -0.7 to -1.5 [which is a reasonable estimate considering the mass-dimensional relations for snow particles reported by Locatelli and Hobbs (1974), Mitchell et al. (1990), Detwiler et al. (1993), Kajikawa (1989), and Brown and Francis (1995)] leads to the change of C_1 of only 10%. Therefore, in spite of the high diversity of ice particle shapes and densities, the relation (27) for determining IWC turns out to be quite stable. Independence of ρ on D leads to a 50% increase in the coefficient C_1.

We can write (27) in a slightly different form:

$$\mathrm{IWC} = CK_{\mathrm{DP}}/(1 - Z_{\mathrm{DR}}^{-1}), \tag{29}$$

where $C = C_1\lambda/30\pi$; that is, the ice water content estimate can be obtained solely from the measurements of K_{DP} and Z_{DR} [expressed in linear scale in (29)]. Because the absolute value of the radar reflectivity factor is not involved, the method is immune to radar calibration errors. For the sake of simplicity, we consider only the case of side incidence; that is, elevation angles are close to zero and there is no canting of particles in the vertical plane. A more detailed analysis shows that elimination of these restrictions has little effect on the $Z_{\mathrm{DP}}/K_{\mathrm{DP}}$ ratio; canting in the vertical plane and/or increase in the elevation angle causes nearly proportional changes in the numerator and the denominator. As a matter of fact, Z_h in (27) is almost independent of the elevation angle γ_0 and the width Ω of the canting angle distribution. Both K_{DP} and Z_{DP} are proportional to the same factors—$\cos^2\gamma_0$ if nonzero elevation angle is considered or $\exp(-2\Omega^2)$ if canting angle distribution is accounted for (Oguchi 1983). Of course, to estimate the ratio reliably, Z_{DP} and K_{DP} must differ sufficiently from zero.

Strictly, the relations (17) and (18) are valid for lightly or moderately aggregated crystals with orthogonal di-

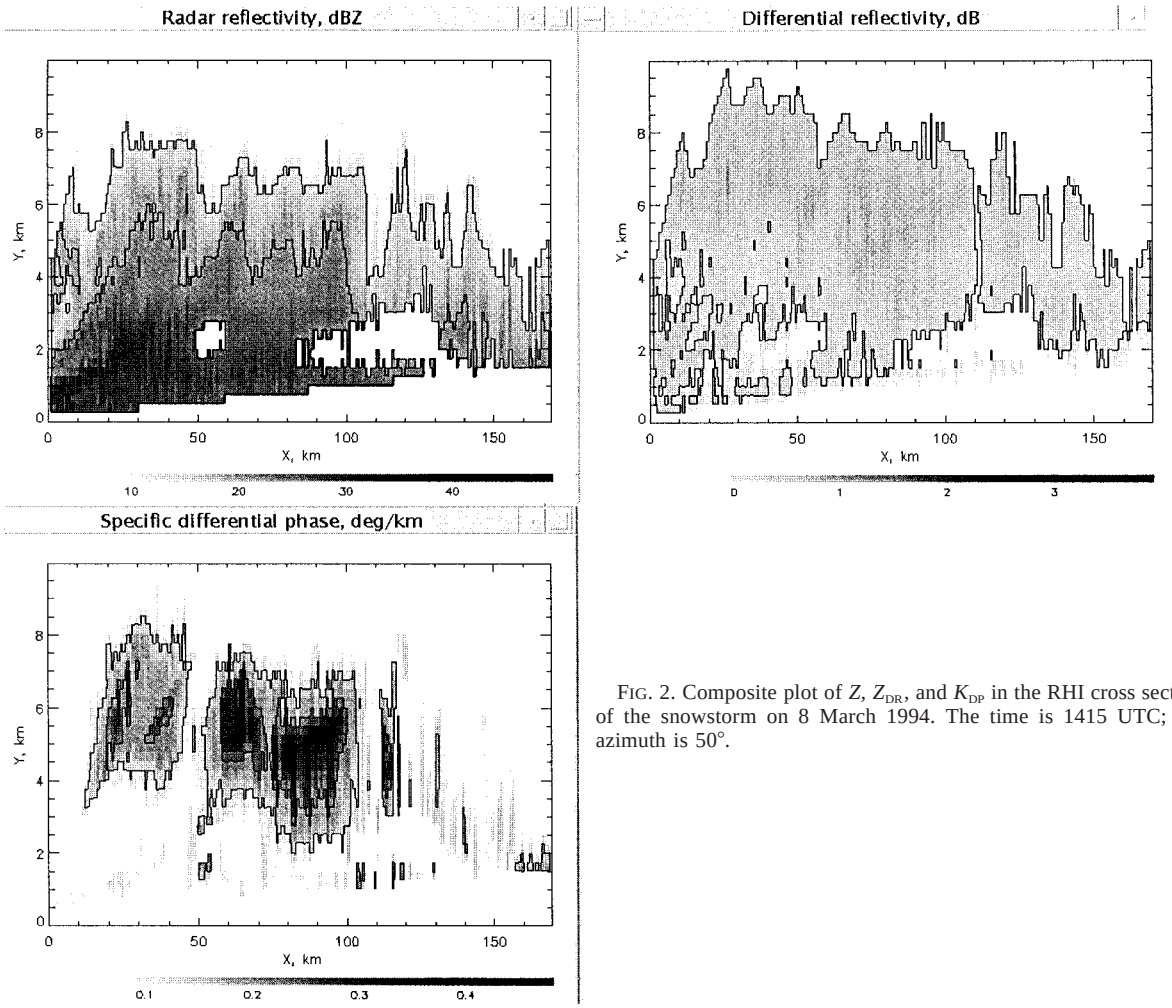

FIG. 2. Composite plot of Z, Z_{DR}, and K_{DP} in the RHI cross section of the snowstorm on 8 March 1994. The time is 1415 UTC; the azimuth is 50°.

mensions specified by (3). However, as aggregation proceeds further, snow particles become more spherical, their orientation becomes more random, and density decreases; hence, the polarimetric contrasts $f_h - f_v$ and $\sigma_h - \sigma_v$ decrease with size, as shown in Fig. 1. This means that the contribution of relatively large aggregates to K_{DP} and Z_{DR} vanishes. Note that this transition from crystals to aggregates does not affect the relation (16) for σ_h. Consequently, the parameter M_0 in (25) still represents the average mass of snow hydrometeors (including both aggregates and crystals). But M_0 in (26) is lower than the true M_0 by an unknown factor $\eta > 1$ because it mainly contains contributions from small-oriented ice crystals. Thus, the right part of (26) should be divided by a factor η. As a result, the coefficient C in the final relation (29) has to be divided by the same factor η if heavy aggregation is present.

At low Z_{DR} the denominator in (29) becomes too small, therefore, even minor errors in Z_{DR} lead to large biases in the IWC estimate. Thus, there is a certain Z_{DR} threshold below which the proposed method is not expected to work well. In the next section, the selection of the threshold is justified by the analysis of the polarimetric data.

4. Experimental evaluation

Measurements of specific differential phase and differential reflectivity made with the NSSL's 10-cm-wavelength polarimetric radar reveal quite large values of K_{DP} and Z_{DR} in thunderstorm anvils and ice parts of winter snowstorms (Ryzhkov and Zrnic 1995). The values of K_{DP} up to 0.8 deg km^{-1} and Z_{DR} up to 3 dB are sometimes observed in the zones of low radar reflectivity (less than 20 dBZ), where elementary or lightly aggregated horizontally oriented crystals comprise the majority of scatterers. The probability of occurrence of large K_{DP} and Z_{DR} increases with increasing height and decreasing air temperature. This vertical dependence of K_{DP} and Z_{DR} is very typical for snowstorms. Figure 2 illustrates vertical cross sections of Z, Z_{DR}, and K_{DP} in the range–height indicator presentation of the snow-

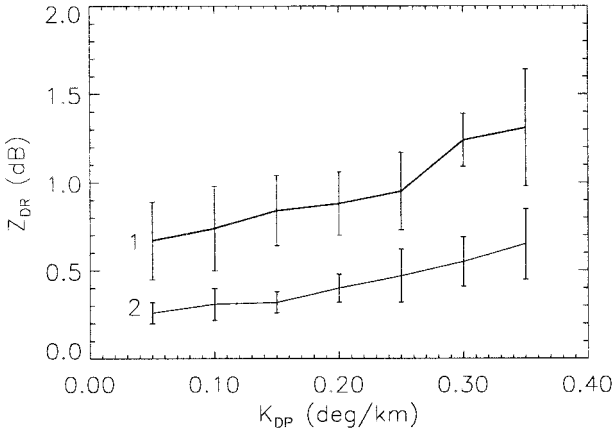

FIG. 3. Average dependencies Z_{DR} vs K_{DP} for two classes of snowstorms (1: ''cold'' snow with $Z < 15$ dBZ, 2: ''warm'' snow with $Z > 15$ dBZ).

storm observed on 8 March 1994 in central Oklahoma. Higher altitudes of the storm are characterized by substantially larger values of K_{DP} and Z_{DR} than near ground, where both polarimetric variables are close to zero due to abundance of low-density aggregates. There is a definite positive correlation between K_{DP} and Z_{DR} that is generally better pronounced at lower temperatures.

To determine what is a relation between K_{DP} and Z_{DR} in snow, we have examined 10 Oklahoma snowstorms that were observed during the period from December 1992 until March 1996. Five are classified as ''cold'' because the surface temperature was below $-5°$C, and pristine or moderately aggregated crystals were the dominant scatterers. These storms have larger Z_{DR} and lower Z for fixed values of K_{DP} than the other five storms that constitute the second class of ''warm'' storms. The rain–snow boundary in the warm storms was near the radar so that both rain and snow precipitation were observed simultaneously within the coverage area. The surface temperatures for warm snowstorms were close or slightly below 0°C, and the storms contained heavily aggregated snow and therefore had larger reflectivities and, on the average, lower K_{DP} and Z_{DR}. The average Z_{DR}–K_{DP} relations for the two classes of snowstorms obtained from analysis of many volume scans of the K_{DP} and Z_{DR} data (for each storm) are plotted in Fig. 3. Because the observed K_{DP} values were of the order of a few tenths or even hundredths of a degree per kilometer, intense filtering had to be applied to the differential phase data to estimate K_{DP}. The choice was a wide running average window over 48 successive range gates (range interval of 7.2 km). The standard deviation of the K_{DP} estimate is about 0.05 deg km^{-1} for this type of averaging (Ryzhkov and Zrnic 1996). Differential reflectivity data were averaged over 24 successive range gates. The resulting standard error in Z_{DR} is about 0.10–0.15 dB (depending on the magnitude of the cross-correlation coefficient). Addititonal spatial averaging of the K_{DP} and Z_{DR} data is performed while transforming the data from polar to rectangular coordinates with a grid resolution of 2 km × 2 km. It is evident from Fig. 3 that in the low-reflectivity cold storms, Z_{DR} is about half a decibel larger for a given K_{DP} than in the warm high-reflectivity snowstorms. The borderline values of Z_{DR} between 0.5 and 0.7 dB separate cold storms (for which the proposed method is expected to work well) from warm storms (for which it is likely to fail). This estimate of the Z_{DR} threshold is subjective and intuitive; a more appropriate criterium can be established by comparing the polarimetric estimates of IWC with in situ measurements. For the typical values of $K_{DP} = 0.2$ deg km^{-1} and $Z_{DR} = 1.0$ dB in cold storms (Fig. 3), the standard errors of the K_{DP} and Z_{DR} measurements cause a fractional standard error in the estimation of IWC of about 40%–45% if the proposed algorithm (29) is used.

A comparison has been performed for the case of 21 May 1995 that was observed during a period of the VORTEX experiment in Oklahoma (Rasmussen et al. 1994). The Cimarron S-band (10-cm wavelength) polarimetric radar detected a region of high K_{DP} aloft in the trailing precipitation behind the squall line that was moving away from the radar (Fig. 4). The radar is located to the left of the precipitation core in Fig. 4. A well-pronounced region of high specific differential phase is centered at the height of 6 km and extends about 20 km in the horizontal direction. The maximum K_{DP} in this region is about 0.6 deg km^{-1} and the maximum Z_{DR} is slightly above 1 dB, whereas the reflectivity factor is less than 25 dBZ. The melting layer, identified from images of Z_{DR} and ρ_{hv} (Figs. 4b,d), is at a height of about 3.0–3.5 km. Note that K_{DP} in the stratiform rain below the melting level is significantly lower than in the ice region aloft.

The instrumented T-28 aircraft of the South Dakota School of Mines and Technology penetrated the region of high K_{DP} at an average altitude of 6.3 km. The aircraft trajectory projected on the conical surface at 4° elevation angle is shown in Fig. 5. Contours and shaded areas are the Z and K_{DP} fields at approximately midflight time. During the penetration flight time of about 20 min, the zone of enhanced K_{DP} moved to the east-northeast, while the temperature of ambient air at the level of cloud penetration was between $-15°$ and $-16°$C. The 2D-P probe data from this height indicate presence of pristine crystals and small aggregates with maximum sizes below 3 mm (see Fig. 6). No graupel or large snowflakes were encountered. Thus, the observed scatterers conform to the basic assumptions of the suggested polarimetric method for IWC determination. Ice water content from the 2D-P probe was computed using the empirical relation between particle mass M and its maximal dimension L (Detwiler et al. 1993):

$$M = 3.41 \times 10^{-2} L^{1.97}, \tag{30}$$

where M is expressed in milligrams and L is in millimeters.

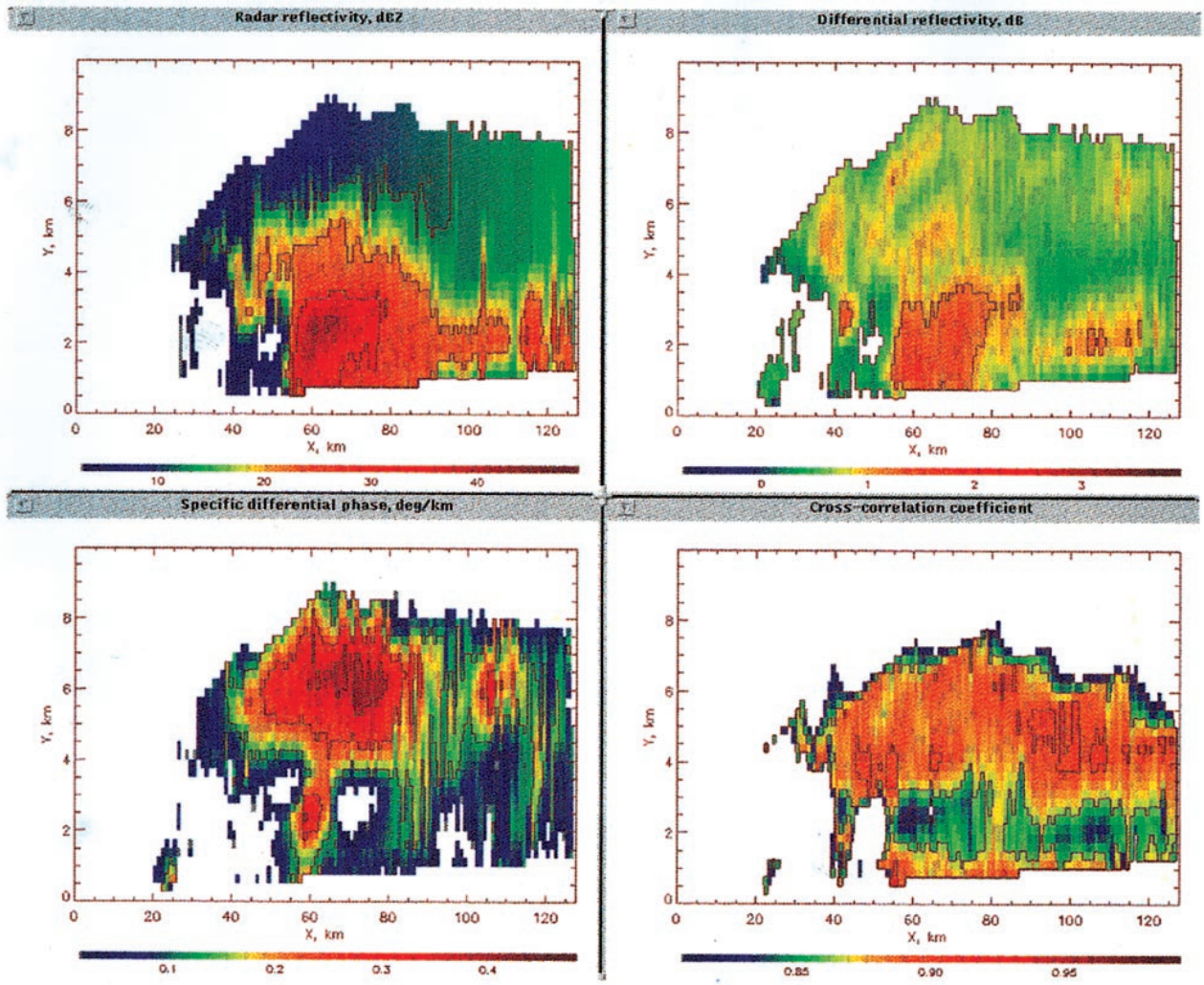

FIG. 4. Composite plot of Z, Z_{DR}, K_{DP}, and ρ_{hv} in the RHI cross section of the storm on 21 May 1995.

Radar polarimetric data along the flight path were reconstructed from four successive volume scans. Between the times of coincident radar and aircraft data, the radar data were extrapolated (advected) forward up to $\Delta_i \mathbf{v}_i/2$ and backward up to $-\Delta_i \mathbf{v}_i/2$ centered on the coincident time t_i; Here, Δ_i is the time between successive volume scans. The advection velocity $\mathbf{v}_i$ was determined from the motion of the 15-dBZ contour at the aircraft height.

Besides the polarimetric method, we also applied two IWC–Z relations. One, IWC $= 0.088Z^{0.58}$, was suggested by Atlas et al. (1995) and represents the best fit for cirrus clouds in the range of reflectivities between -50 and 10 dBZ. The other relation, IWC $= 0.035Z^{0.51}$, suggested by Heymsfield (1977), summarizes the results obtained for stratiform ice clouds in the Z interval between -15 and 25 dBZ. The latter relation is close to the one recently obtained by Thomason et al. (1995) for aggregating snow particles (IWC $= 0.034Z^{0.40}$).

Two variants of the polarimetric algorithm are tested. In one, the differential reflectivity is set to 0.7 dB in (29) for data that have $Z_{DR} < 0.7$ dB so that IWC $= 3.22K_{DP}$ applies in areas of low differential reflectivity. In the second variant, the formula IWC $= 3.22K_{DP}$ is used throughout. Note that this is almost identical to IWC $\approx 3K_{DP}$ that ensues from the basic formula (18) in Vivekanandan et al. (1994):

$$K_{DP} = \frac{47.4}{\lambda}(1 - r)^{1.2}\rho^{-0.033}\text{IWC}, \tag{31}$$

in which the axis ratio r is set to 0.2 and $\lambda = 109.7$ mm. Although different assumptions are behind the two approaches, the similarity of results is only for an axis ratio of 0.2. This might not be a chance coincidence considering that 0.2 is about the average of axis ratios for the six types of crystals ($L > 0.5$ mm) reported by Matrosov (1991, Fig. 1). We believe that in regions of

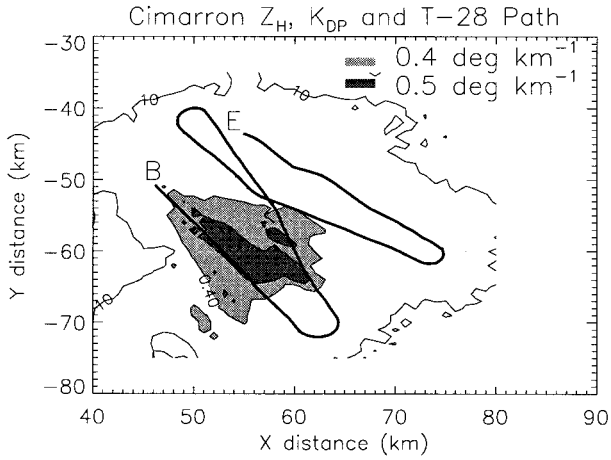

FIG. 5. The T-28 aircraft flight path in the observational area of the storm. Shaded areas represent the zones of K_{DP} exceeding 0.4 and 0.5 deg km^{-1}; the contour labeled with 10 encircles the area where Z is over 10 dBZ. The B and E correspond to the beginning (14:29:20) and ending (14:49:00) locations of the aircraft. Only the first two-thirds of the first NW-SW flight leg are compared with the radar data presented in this figure; later volume scans are used to compare the remainder of the T-28 measurements.

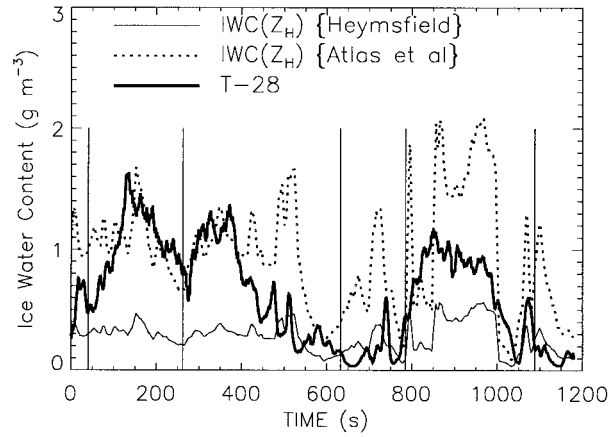

FIG. 7. Comparison of the results of in situ measurements of IWC (thick solid line) with the IWC estimates derived from radar reflectivity data using two IWC–Z relations (thin, solid, and dotted lines). The vertical lines are at the times when the location of the T-28 aircraft and the region the Cimarron radar antenna was scanning are coincident.

differential reflectivity higher than about 1 dB, use of the joint K_{DP}–Z_{DR} algorithm (29) is more appropriate (see the K_{DP}–Z_{DR} curve for cold snowstorms in Fig. 3).

Ice water content computed from the measurements on board the T-28 aircraft and the radar estimates are illustrated in Figs. 7 and 8. The aircraft data have been uniformly averaged over 9 s. Vertical lines on these figures indicate coincident times of the in situ and radar observations; between these times, the radar data had been extrapolated as previously explained. For the Atlas et al. relation, considerable overestimation of the actual IWC is seen in the period between 800 and 1000 s. This could be partly due to the fact that radar data from two elevations were spliced because the elevation at which the aircraft path was centered was changing from 3.8° to 3.2° and back to 3.8°, whereas scans were made at 3° and 4°. From about 100 to 400 s, the Atlas et al. relation agrees very well with the in situ measurements, whereas Heymsfield's algorithm shows significant underestimation of actual IWC. This is somewhat unexpected because the observed Z's of 15–24 dBZ fit the range for which Heymsfield's (1977) relation is supposed to be valid and are outside the region for which the Atlas et al. (1995) formula was derived. Correlation coefficients between the in situ and radar-derived IWC are 0.52 and 0.51, whereas the rms differences are 0.50 g m^{-3} and 0.55 g m^{-3} for the Atlas et al. and the Heymsfield formulas. As can be seen (Fig. 7), the differences between in situ and radar measurements at and in between the coincidence times are not systematic. We, therefore, speculate that the spatial sampling and sensitivity of the IWC–Z relation might be significant causes of the differences.

The polarimetric algorithms yield better agreement with in situ measurements (Fig. 8) than the algorithms that use the IWC–Z relations (Fig. 7). The correlation coefficients between the in situ and radar-derived IWC are 0.62 and 0.69, whereas the rms differences are 0.46 g m^{-3} and 0.40 g m^{-3} for the IWC(K_{DP}) and IWC(K_{DP}, Z_{DR}) methods. The polarimetric estimate of the IWC has a positive bias of about 0.26 g m^{-3} and a standard error of 0.4 g m^{-3} for this particular case. Note that inclusion of Z_{DR} slightly improves the agreement between the in situ and radar estimate of IWC. Again, we conclude that time coincidence, or lack thereof, is not a major contributor to the difference between in situ and radar-de-

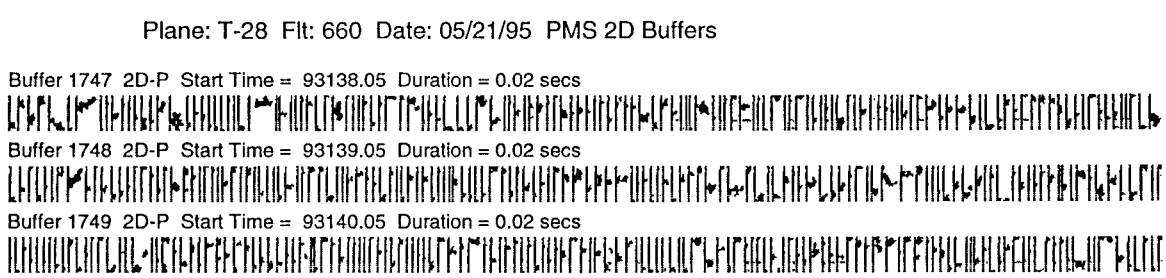

FIG. 6. An example of 2D-P images for the data collected on board the T-28 aircraft. The bar length corresponds to 6.4 mm.

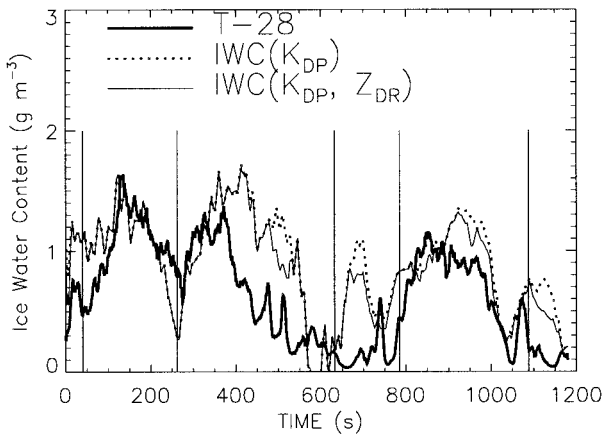

FIG. 8. Comparison of the results of in situ measurements of IWC (thick solid line) with the IWC estimates derived using K_{DP} (dashed line) and the joint K_{DP} and Z_{DR} measurements (thin solid line).

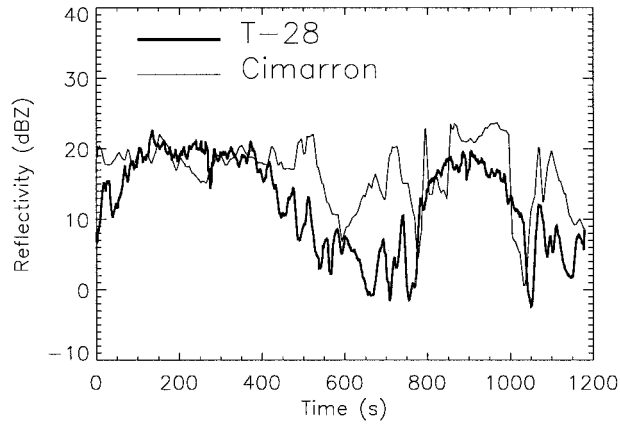

FIG. 9. Reflectivity factor estimated from the in situ measurements and the radar.

rived IWCs. Because both polarimetric algorithms capture well the variations of the IWC, we submit that in this case these algorithms are less sensitive to variations of ice crystal distributions and shapes. The limited amount of data precludes identification of the major reasons for the difference between the in situ and polarimetric measurements. Still, unequal sampling probably plays a significant role, and further comparisons with in situ data are needed before more definite conclusions can be made.

To check bias and sampling errors, we compared the reflectivity factor measured by the radar and the one computed from the 2D-P probe data (Fig. 9). The reflectivity factor Z from the 2D-P probe was determined using the relation (19). With $a_1 = 7.3$ and $K^2 = 0.928$, the formula for Z is

$$Z = 0.87 \sum M^2(L_i)N(L_i), \tag{32}$$

where L_i is the maximal dimension of the particle (3), N is the concentration of particles in the ith size category, and $M(L_i)$ is the mass obtained from (30). In (32), Z is expressed in mm^6 m^{-3}, M is in mg, and N is in m^{-3}. As can be seen from Fig. 9, the in situ and radar estimates of the reflectivity factor are in reasonably good agreement, especially at larger reflectivities, in spite of large differences in sampling volumes and evolution of particles between the times of coincidence.

Given the accuracy of K_{DP} estimates achievable at the 10-cm wavelength, our results suggest that reasonable estimates of IWC should be possible for IWC exceeding about 0.1 g m^{-3}. To quantify lower IWCs using a similar technique, shorter radar wavelengths are needed.

5. Conclusions

The weakness of current methods for IWC determination from reflectivity factor measurements is in the fact that the radar reflectivity is a product of IWC and the average mass of scatterers. Thus, one more independent measurement is needed for estimating IWC. Such measurement can be provided by a polarimetric radar. We have shown that the ratio between the reflectivity difference $Z_{DP} = Z_h - Z_v$ and the specific differential phase K_{DP} is a good estimator of the mass of the average-sized pristine or moderately aggregated ice crystals.

Modeling was performed taking into account different shape and density dependencies on the size of scatterer for 11 categories of ice crystals consisting of three oblate and eight prolate types. It is shown that the ratio Z_{DP}/K_{DP} is practically insensitive to the shape and density of ice hydrometeors and is determined by their average mass. The combination of Z_h and Z_{DP}/K_{DP} yields a simple formula for IWC as a function of K_{DP} and Z_{DR} with the coefficient of proportionality virtually not affected by the ice particles' shape or density.

For heavily aggregated snow hydrometeors, the suggested method is expected to be less reliable and likely overestimates the actual ice water content. This is because polarimetric contrasts in K_{DP} and Z_{DR} are vanishingly small for large aggregates that have low density, nearly spherical shape, and tumble while falling.

Experimental check of the proposed method was made using in situ 2D-P data collected on board the T-28 aircraft during penetration into an ice cloud. In this case, where pristine and moderately aggregated crystals constitute the majority of scatterers, the polarimetric algorithms exhibited a noticeably better performance than two IWC–Z relations. Ice water content in the range above 0.1 g m^{-3} was correctly quantified with an S-band polarimetric radar. Addititonal in situ data are needed for verification of the proposed method.

Acknowledgments. The authors are grateful to Dr. J. Straka from the University of Oklahoma who was instrumental in securing participation of the T-28 aircraft. Dr. A. Detwiler and K. Hartmann from the South Dakota School of Mines and Technology provided the 2D-P

aircraft data and were helpful in the 2D-P data analysis. We appreciate useful comments of Dr. S. Y. Matrosov from the Environmental Technology Laboratory. M. Schmidt and R. Wahkinney have maintained and calibrated the Cimarron polarimetric radar. The T-28 operation was supported by the National Science Foundation Division of Atmospheric Sciences lower atmospheric research facilities deployment pool. The research assistantship of B. Gordon was partly supported by NSF Grant ATM-9311911 and by NASA through agreement with NOAA S-64075-E.

REFERENCES

Atlas, D., S. Y. Matrosov, A. J. Heymsfield, M.-D. Chou, and D. B. Wolff, 1995: Radar and radiation properties of ice clouds. *J. Appl. Meteor.,* **34,** 2329–2345.

Auer, A. H., and D. L. Veal, 1970: The dimension of ice crystals in natural clouds. *J. Atmos. Sci.,* **27,** 919–926.

Aydin, K., and C. Tang, 1995: Estimation of ice water content with 94-GHz millimeter wave radar observables. Preprints, *27th Conf. on Radar Meteorology,* Vail, CO, Amer. Meteor. Soc., 550–552.

Brown, P., and P. Francis, 1995: Improved measurements of the ice water content in cirrus using a total-water probe. *J. Atmos. Oceanic Technol.,* **12,** 410–414.

Detwiler, A. G., N. C. Knight, and A. J. Heymsfield, 1993: Magnitude of error factors in estimates of snow-particle masses from images. *J. Appl. Meteor.,* **32,** 804–809.

Heymsfield, A. J., 1972: Ice crystal terminal velocities. *J. Atmos. Sci.,* **29,** 1348–1357.

——, 1977: Precipitation development in stratiform ice clouds: A microphysical and dynamical study. *J. Atmos. Sci.,* **34,** 367–381.

Jayaweera, K. O. L. F., and R. E. Cottis, 1969: Fall velocities of plate-like and columnar ice crystals. *Quart. J. Roy. Meteor. Soc.,* **95,** 703–709.

——, and T. Ohtake, 1974: Properties of columnar ice crystals precipitating from layer clouds. *J. Atmos. Sci.,* **31,** 280–286.

Kajikawa, M., 1989: Observation of the falling motion of early snowflakes. Part II: On the variation of falling velocity. *J. Meteor. Soc. Japan,* **67,** 731–737.

Locatelli, J. D., and P. V. Hobbs, 1974: Fall speeds and masses of solid precipitation particles. *J. Geophys. Res.,* **79,** 2185–2197.

Matrosov, S. Y., 1991: Theoretical study of radar polarization parameters obtained from cirrus clouds. *J. Atmos. Sci.,* **48,** 1062–1070.

——, R. F. Renking, R. A. Kropfli, and B. W. Bartram, 1996: Estimation of ice hydrometeor types and shapes from radar polarization measurements. *J. Atmos. Oceanic Technol.,* **13,** 85–96.

Mitchell, D. L., R. Zhang, and R. L. Pitter, 1990: Mass-dimensional relationships for ice particles and the influence of riming on snowfall rates. *J. Appl. Meteor.,* **29,** 153–163.

Oguchi, T., 1983: Electromagnetic wave propagation and scattering in rain and other hydrometeors. *Proc. IEEE,* **71,** 1029–1078.

Pruppacher, H. R., and J. D. Klett, 1978: *Microphysics of Clouds and Precipitation.* D. Reidel, 714 pp.

Rasmussen, E. N., J. R. Straka, R. Davies-Jones, C. A. Doswell III, F. H. Carr, M. D. Eilts, and D. R. MacGorman, 1994: Verification of the Origins of Rotation in Tornadoes Experiment: VORTEX. *Bull. Amer. Meteor. Soc.,* **75,** 1007–1017.

Ryzhkov, A. V., and D. S. Zrnic, 1995: Polarimetric measurements of snow. Preprints, *27th Conf. on Radar Meteorology,* Vail, CO, Amer. Meteor. Soc., 458–460.

——, and ——, 1996: Assessment of rainfall measurement that uses specific differential phase. *J. Appl. Meteor.,* **35,** 2080–2090.

Sassen, K. D., 1987: Ice cloud content from radar reflectivity. *J. Appl. Meteor.,* **26,** 1050–1053.

Sekhon, R. S., and R. C. Srivastava, 1970: Snow size spectra and radar reflectivity. *J. Atmos. Sci.,* **27,** 299–307.

Thomason, J. W. G., A. J. Illingworth, and V. Marecal, 1995: Density and size distribution of aggregating snow particles inferred from coincident aircraft and radar observations. Preprints, *27th Conf. on Radar Meteorology,* Vail, CO, Amer. Meteor. Soc., 127–129.

van de Hulst, H. C., 1981: *Light Scattering by Small Particles.* Dover Publications, 470 pp.

Vivekanandan, J., V. N. Bringi, M. Hagen, and P. Meischner, 1994: Polarimetric radar studies of atmospheric ice particles. *IEEE Trans. Geosci. Remote Sens.,* **32,** 1–10.